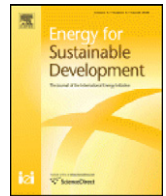




Contents lists available at SciVerse ScienceDirect

Energy for Sustainable Development



Estimating the spatial distribution of woody biomass suitable for charcoal making from remote sensing and geostatistics in central Mexico

Miguel Ángel Castillo-Santiago^{a,*}, Adrián Ghilardi^{b,c}, Ken Oyama^d, José Luis Hernández-Stefanoni^e, Ignacio Torres^d, Alejandro Flamenco-Sandoval^f, Ana Fernández^b, Jean-François Mas^b

^a Laboratorio de Análisis de Información Geográfica y Estadística, El Colegio de la Frontera Sur, Carretera Panamericana y Periférico sur s/n., San Cristóbal de las Casas CP 29290, Chiapas, Mexico

^b Centro de Investigaciones en Geografía Ambiental (CIGA), Universidad Nacional Autónoma de México (UNAM), antigua carretera a Pátzcuaro 8701, Morelia CP 58190, Michoacán, Mexico

^c School of Forestry and Environmental Studies, Yale University, 195 Prospect Street, 06511, New Haven, CT, USA

^d Centro de Investigaciones en Ecosistemas (CIEco), Universidad Nacional Autónoma de México (UNAM), antigua carretera a Pátzcuaro 8701, Morelia CP 58190, Michoacán, Mexico

^e Unidad de Recursos Naturales, Centro de Investigación Científica de Yucatán A.C., Calle 43 # 130, Mérida CP 97200, Yucatán, Mexico

^f Departamento de Ingeniería Geomática e Hidráulica, Universidad de Guanajuato, Av Juárez 77, Guanajuato CP 36000, Guanajuato, Mexico

ARTICLE INFO

Article history:

Received 16 August 2012

Revised 16 October 2012

Accepted 16 October 2012

Available online xxx

Keywords:

Charcoal

Aboveground biomass

Geostatistics

SPOT5 images

Quercus spp.

Cuitzeo basin

ABSTRACT

We present a cost-effective statistical approach that integrates satellite imagery, environmental variables and ground inventory data to map the spatial distribution of aboveground woody biomass suitable for charcoal making. The study was conducted in the Cuitzeo basin located in central Mexico, where charcoal is produced from oak forests covering approximately 10% of the total area (4033 km²). Diameters of trees and sprouts in 78 plots of 0.2 ha each was measured. Allometric equations previously developed locally that only require tree diameters were employed to estimate the amount of woody biomass suitable for charcoal making i.e. the amount of wood that is loaded into the kilns. The performance of two statistical techniques for the interpolation of field data was assessed by cross-validation; these techniques were linear regression and regression-kriging, the second taking into account the spatial autocorrelation of data. Spectral bands, vegetation indices, texture measurements and variables derived from a Digital Elevation Model were examined as explanatory variables. Accounting for spatial autocorrelation (regression-kriging) improved the model's R^2 from 0.61 to 0.69, representing a relative error reduction of 11.3% (from 11.01 to 9.77 t ha⁻¹ of wood suitable for charcoal). The available stock was compared to current estimates of charcoal demand in the Cuitzeo basin and insights were given on how this information can be used to estimate the annual sustainable production potential of oak in order to account for supply–demand balances.

© 2012 Elsevier Inc. All rights reserved.

Introduction

Woody biomass is one of the main sources of energy for food preparation and heating for millions of poor households in developing countries (FAOstat, 2010; IEA, 2006, 2012; Parikka, 2004). While fuelwood use worldwide seems to have achieved a plateau, charcoal production for residential and commercial purposes i.e. non-industrial, will keep rising in the following decades, driven mainly by urban and peri-urban growth in developing countries, mostly in Sub-Saharan Africa (Arnold et al., 2003, 2006; FAOstat, 2010). The urban demand for charcoal responds in turn to its preference as a cooking fuel as

compared to fuelwood (Emrich, 1985; von-Jonstorff and Nagel, 2010), as it emits less smoke, even when using traditional stoves (Johnson et al., 2011; Naughton-Treves et al., 2007; Pennise et al., 2001).

Charcoal production is identified as a major cause of deforestation and forest degradation (e.g. Ahrends et al., 2010; Hofstad, 1997; Mwampamba, 2007; Zulu, 2010). In some critical areas, charcoal constitutes by far the main product of forest removals. It is also the main source of cooking energy of urban dwellers (e.g. up to 80% in some southern African nations Stockholm Environment Institute, 2002). Interventions to limit or ban it are rarely successful because of the intensity of urban market demand for this product (Mwampamba, 2007). Attempts to introduce more efficient charcoal kilns have in many cases failed, largely because of lack of understanding of the real economics of charcoal production and of contextual factors that limit charcoal producers' options (Khundi et al., 2011). Nevertheless, under sound management practices of forests and woodlands, charcoal production can be environmentally neutral and significantly contribute to satisfy the energy needs of the rural population, to generate employment and to reduce poverty (Hansfort and Mertz, 2011). On

Abbreviations: WSC, above-ground woody biomass suitable for charcoal making.

* Corresponding author. Tel.: +52 967 674 9000x1854; fax: +52 967 674 9021.

E-mail addresses: mcastill@ecosur.mx (M.Á. Castillo-Santiago),

aghilardi@ciga.unam.mx, adrian.ghilardi@yale.edu (A. Ghilardi),

akoyama@oikos.unam.mx (K. Oyama), jl_stefanoni@cicy.mx

(J.L. Hernández-Stefanoni), itorreg@oikos.unam.mx (I. Torres), flamenco@ugto.mx

(A. Flamenco-Sandoval), anafernandez03@gmail.com (A. Fernández),

jfmas@ciga.unam.mx (J.-F. Mas).

0973-0826/\$ – see front matter © 2012 Elsevier Inc. All rights reserved.

<http://dx.doi.org/10.1016/j.esd.2012.10.007>

Please cite this article as: Castillo-Santiago M.Á., et al., Estimating the spatial distribution of woody biomass suitable for charcoal making from remote sensing and geostatistics in central..., Energy for Sustainable Development (2012), <http://dx.doi.org/10.1016/j.esd.2012.10.007>

the contrary, when stakeholders' interests along the commodity chain are driven by large charcoal profits, negative environmental impacts are expected. Usually, abandoned, non-productive or poorly guarded forests and woodlands are leased to—or plundered by—charcoal producers whose production rate does not allow for natural regeneration or sprouting, their exploitation areas gradually expanding away from demand centers. Shortened cycles of clear-cutting combined with inefficient kilns, grazing and altered fire regimes can ultimately lead to severe forest degradation i.e. forests presenting a decreased wood productivity, soil sterilization, higher incidence of pests and inhibition of sexual reproduction, among other signs of alteration. Eventually, deforestation or even long-term desertification can occur.

It is in this sense that the spatial distribution of above-ground woody biomass suitable for charcoal making (WSC) represents a highly desirable piece of information for designing improved management practices. For example, it allows for spotting degrading areas (e.g. Ryan et al., 2012) as well as mapping below-than-expected biomass where a biophysical potential for cost-effective management can exist i.e. where there is room to growth (e.g. Paradzayi and Annegarn, 2012).

Mapping biomass stocks or other structural attributes of vegetation has traditionally been made based on maps of vegetation type or land cover, usually estimating the mean value of each thematic class by means of field measurements in locations. This approach has limitations due to the subjectivity involved in the delimitation of thematic classes and the estimation of values for a single factor of interest within the same land cover class (Goetz et al., 2009), which means that the method does not consider variability within the class. In the case of managed forests the assumption of within-class homogeneity becomes unlikely given that, added to the natural variability of forests derived from different soil and topography conditions, biomass extraction creates a further heterogeneous structure for a given vegetation type.

An alternative approach for mapping forest structure attributes and biomass stocks in large areas is the use of remotely sensed data calibrated with field information. This method is based on the association between areal forest biomass and spectral properties of the corresponding space-borne imagery (Avitabile et al., 2011; Im and Gleason, 2011; Lu, 2006; Paradzayi and Annegarn, 2012; Ryan et al., 2012). Once field and image data are empirically calibrated, their relation is used to assess values for variables of interest outside sampled sites i.e. over all pixels in the image. An additional advantage of applying this approach is the capacity of obtaining continuous maps of the variable of interest at relatively low cost depending on the image resolution and the spatial and time coverage of the data available.

Among the methods used for image calibration are linear regression (Castillo-Santiago et al., 2010; Lu, 2006), K nearest neighbor (Lasserre et al., 2011) or neural networks (Foody et al., 2001). The more commonly used spectral properties of satellite images are spectral vegetation indices, reflectance of selected bands, or transformations of these by procedures such as principal component analysis. With the increasing availability of images having higher spatial resolution, image texture analysis has become an important tool for obtaining explanatory variables in some biomass models (Lu and Batistella, 2005). Image texture is the tonal variation of spatial domains expressed as the roughness or smoothness of a given region of the image (Lillesand and Kiefer, 1994), which is in general associated to the type of land cover. The inclusion in forest biomass estimation models of variables such as texture incorporates spatial information contained in satellite images. Although satellite data are in many cases sufficient for estimating the spatial distribution of biomass with a low level of uncertainty, the incorporation of additional environmental variables such as slope or solar radiation may increase the predictive capability of models due to the close relation between these variables and the structure of forests (Clark and Clark, 2000).

The above-mentioned methods for estimating biomass have not explicitly taken into account the spatial dependency of field data,

because independence is assumed by means of a careful sampling design statistically. However, when dealing with vegetation, neighboring sites generally are more similar in vegetation structure than distant sites; this means that they are spatially autocorrelated. Because of this fact, spatial independence is one of the most difficult assumptions to fulfill, given that most ecological and environmental processes display a pattern of spatial dependency or autocorrelation (Legendre, 1993).

On the other hand, the geostatistical methods explicitly model the data structure of spatial autocorrelation and incorporate this information in the estimation of the variable of interest for unsampled locations. Some of these methods additionally make use of auxiliary data more exhaustively gathered for the area of interest, such as satellite images. There are several geostatistical methods that use auxiliary data, among which are universal kriging, cokriging, kriging with external drift and regression-kriging (RK) (Hengl et al., 2007). The above-mentioned methods differ in the way they use the auxiliary information in order to estimate the variable of interest in unsampled areas. Recent studies have shown the superiority of RK when compared to the other two methods (Hernandez-Stefanoni et al., 2011). RK combines a linear regression method with the ordinary kriging of the residuals of the regression.

In this study we present a cost-effective statistical approach that integrates satellite imagery with ground inventory data to map the spatial distribution of aboveground woody biomass suitable for charcoal making. The improvement in the accuracy of estimation was analyzed by adding a geostatistical model accounting for the autocorrelation of residuals. The available stock was compared to current estimates of charcoal demand in the study area (the Cuitzeo basin) and insights were given on how this information can be used to estimate the annual sustainable production potential of oak wood in order to account for supply–demand balances.

Methods

Study area

The Cuitzeo basin is located in the Trans-Mexican Volcanic Belt (Fig. 1), spanning from 19°30' to 20°05' north latitude and from 100°35' to 101°30' west longitude, covers an area of 4033 km². The basin's name comes from lake Cuitzeo, a body of water located in the lower portion of the basin with an extension of 242 km² (Mendoza et al., 2006). Precipitation in the Cuitzeo basin increase from south to north with an annual average of 765 mm, as does temperature, with an annual average of 14.4 °C (García, 2004). The spatial distribution of rainfall and temperature—both having a seasonal behavior (Mendoza et al., 2005)—indicates that the study area is located in a transitional zone between the dry temperate and the humid temperate climates.

The study area was originally covered by temperate oak (*Quercus* spp.) and pine (*Pinus* spp.) mixed forests, which at present cover 20% of the total surface of the catchment. The main land uses are rainfed agriculture and grasslands, covering about 50% of the basin (Mendoza et al., 2011).

The Cuitzeo basin is a densely populated area (254 inhabitants km⁻²). Nearly one million people live in the basin, of which 80% live in urban settlements and 66% in the cities of Morelia and Zinapécuaro de Figueroa (INEGI, 2011). The basin's urban population (charcoal is not used in rural areas), grew 330% between 1970 and 2010 (INEGI, 2010). The environmental and socioeconomic conditions in the Cuitzeo basin are representative of those in Central Mexico (López et al., 2006).

Oak forests in the Cuitzeo basin are regularly clear-cut for illicit charcoal production i.e. without approved forest management programs (Ghilardi et al., in preparation). However, how much oak charcoal is burned in the Cuitzeo Basin? Two preliminary reference values exist so far. A study by Masera et al. (2010) that reported a consumption of 14000 tCh (metric tons of charcoal) for the whole state of

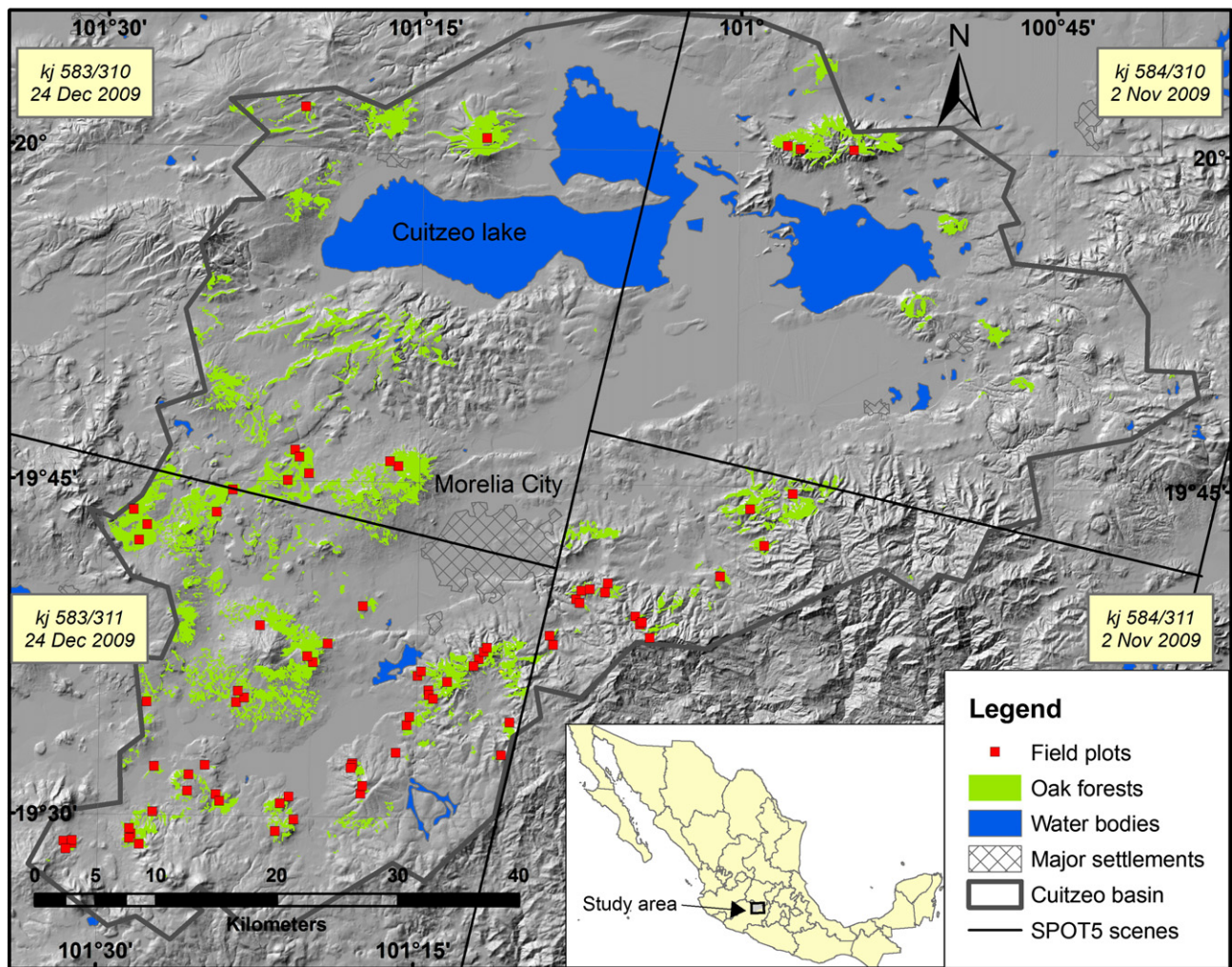


Fig. 1. Location of the Cuitzeo basin showing the relief, the spatial distribution of sampling sites, the patches of oak forest and the areas covered by the SPOT 5 images analyzed with their corresponding acquisition dates.

Michoacán—where most of the Cuitzeo basin belongs—equivalent to 7778 tDMeq (equivalent metric tons of woody biomass in dry matter or equivalent woody biomass suitable for charcoal making (WSC)), assuming an average yield of kilns of about 18% (half that measured in the study area of 31% (Ghilardi et al., in preparation)). Urban population in the Cuitzeo basin represents 26% of the State's urban total (INEGI, 2010), so we can estimate a basin's consumption of about 3640 tCh, or an equivalent in dry woody biomass (WSC) between 11742 to 20222 t depending on the assumed kiln's yield: 31% to 18% respectively.

The second reference comes from an ongoing study in which a survey on charcoal use by the residential sector only (sample size = 309 households, stratified by income class) have been conducted in the city of Morelia (Ghilardi et al., in preparation). The extrapolated value for the whole city is around 2270 tCh, and for the entire basin is 2806 tCh (WSC = 9052–15590 t), not considering packed and branded charcoal that necessarily comes from outside the study area as a forest management registry is needed for branding and commercialization. The residential charcoal consumption could be about 50% to 75% of total consumption which include restaurants and street food vendors. Total consumption should range between 11,315 (9052 × 1.25) and (15590 × 1.50) 23385 t of WSC. Both independent studies estimates coincide fairly well, although the second one only considers non-branded charcoal (i.e. the first one must be a sub estimation) and is still ongoing meaning that the uncertainty range will be narrowed in the end. Fig. 2 shows some examples within the

study area of clearing activities for charcoal making followed by the coppicing of oaks.

Field data

A total of 78 georeferenced plots of 0.2 ha each (20 × 100 m) were established between 2007 and 2009. A collection of 18 variables were recorded for each oak sprout within a plot, among these variables two are relevant for this study: species (of the stool) and diameter at breast height (dbh), corresponding to 1.30 m of height. To estimate the above-ground woody biomass suitable for charcoal making (WSC), a set of four previously constructed allometric equations in the form $y = a(\text{dbh})^b$ were used; three of them correspond to the most abundant oak species in the region (*Q. castanea*, *Q. laeta*, and *Q. deserticola*¹) and a fourth generic equation was used for the remaining oak species (Aguilar et al., 2012). These equations were built in the same study area using destructive sampling and working with local charcoal producers. For larger trees (dbh > 38.1 cm), a new set of linear equations in the form $y = a + b(\text{dbh})$ were fitted for this study, using the same

¹ The mentioned reference reports both the allometry and growth rates for *Q. castanea* and *Q. laeta*. Only the allometry was estimated for *Q. deserticola* so it was not reported in Aguilar et al. (2012) for the sake of consistency.



Fig. 2. Cleared patches for charcoal making followed by coppicing in oak forests and rangelands in the Cuitzeo basin. Note: Images are shown as a visual reference only; they were saved from GoogleEarth and are not orthorectified. The scale bar is approximate.

dataset. This was done in order to avoid overestimating the volumes of larger—although scarce— oak sprouts. All the allometric equations used here can be consulted in the online supplementary material.

Remote sensing and GIS data

We used panchromatic and multispectral SPOT5 images. Complete mapping of the study area was obtained by two trajectories of this

satellite, the first one, scenes KJ 584/310 and 584/311, was acquired on November 2, 2009 and covered approximately 40% of the study area; the second one, scenes KJ 583/310 and 583/311, was acquired on December 24, 2009 covering the remaining area (see Fig. 1). The SPOT-5 multispectral images are made up of 4 bands (green: 0.50–0.59 μm , red: 0.61–0.68 μm , near infrared (NIR): 0.78–0.89 μm and mid infrared (MIR): 1.58–1.75 μm) with a spatial resolution of 10 m (except MIR whose nominal resolution is 20 m). The spatial resolution of the panchromatic image (Pan: 0.48–0.71 μm) is 2.5 m.

Scenes were orthorectified using ground control points, after which atmospheric correction was made using the Fast Line-of-sight Atmospheric Analysis of Spectral Hypercube (FLAASH) module that is based on MODTRAN4 (ITT, 2006). The geometrically and atmospherically corrected panchromatic and multispectral images were used for calculation of the Normalized Difference Vegetation Index (NDVI) (Tucker, 1979) and first and second order texture values, which were determined in 7×7 pixels windows (Haralick et al., 1973). Texture and window size statistics were set based on the results of Castillo-Santiago et al. (2010), who reported maximum texture and biomass correlation levels in SPOT5 images when using variance and dissimilarity in windows sized 7×7 , 9×9 and 11×11 pixels.

A Digital Elevation Model (DEM) obtained from contour lines interpolation with a 30-m resolution was used for generating slope and annual solar radiation layers. Derived variables were classified in three groups: spectral (the five SPOT5 bands plus NDVI), textural (variance and dissimilarity) and topographic (elevation, slope and solar radiation). All DEM originated variable layers were resampled to the pixel size of SPOT5 multispectral images (10 m).

Plot polygons were digitized based on GPS recorded vertices and overlaid to satellite images. Pixels totally included inside polygons were extracted and used for model calibration. Finally, an interpolation mask was generated by the digitalization of oak forest distribution on the satellite images.

Linear regression analysis

Linear regression (LR) and adjustment by means of simple ordinary least squares (OLS) has been one of the most frequently used statistical approaches to modeling the correspondence between spectral and field data (Lu, 2006). There is an ample literature and tests allowing for verifying assumptions of the regression model are met: normality of residuals, homoscedasticity and absence of multicollinearity. It is generally assumed that data independence is achieved by means of an adequate sampling design.

In search for the most parsimonious model built with easily understood variables, models having a limited number of regressors were analyzed trying to incorporate into the model at least one variable from each type (spectral, textural and topographic). The contributions of each independent variable or sets of variables to increase the percentage of variance explained were examined.

Due to the relatively large plot size (2000 m^2) and in order to avoid heterogeneous pixels in the regression analysis, it became necessary to verify that plots did not present more than one condition i.e. that each plot showed a similar forest structure within. Such heterogeneous conditions were detected through an analysis of influential points (outliers). Outliers were identified aided with a graphic combining studentized residuals, hat values and Cook distance using the *car* package (Fox and Weisberg, 2011) in the software R (R Development Core Team, 2012), and plots of partial residuals (Larsen and McCleary, 1972). The latter tool additionally allowed for a graphic evaluation of linearity and relative contribution of modeled variables.

Also applied statistical tests were normality (Shapiro–Wilk) and homoscedasticity of residuals (Breush–Pagan), calculation of variance inflation factors was made to detect possible problems of multicollinearity between independent variables. In order to eliminate heteroscedasticity

or lack of normality of residuals issues, transformations of dependent variables were assayed.

Geostatistical analysis

It is proposed that any value of the objective variable Z present in a locality s can be modeled as the sum of a deterministic component $m(s)$, a random spatially autocorrelated component $\varepsilon'(s)$ and a pure noise component:

$$Z(s) = m(s) + \varepsilon'(s) + \varepsilon'' \quad (1)$$

The deterministic component $m(s)$, also known as deterministic trend, can be modeled using linear regression, while the random component—in practice equivalent to the residuals of the regression—is modeled using traditional geostatistical tools such as variograms and kriging interpolation, so that any estimated \hat{z} value for an unexplored site s_0 is estimated as (Hengl et al., 2007):

$$\hat{z}(s_0) = \sum_{k=0}^p \hat{\beta}_k \cdot q_k(s_0) + \sum_{i=1}^n \lambda_i \cdot e(s_i) \quad (2)$$

where $\hat{\beta}_k$ corresponds to the adjusted parameters of the regression model; p is the number of auxiliary predictors or variables, q is the predictor variables, λ_i corresponds to kriging weights determined by the spatial dependence structure and $e(s_i)$ is the residual of the regression model in site s_i .

Once the structure of the regression model was established for both SPOT dates, predicted and residual values were calculated, making sure that these values met the assumptions of normality and homoscedasticity and tests were applied to these data to determine the structure of the empirical variograms. Anisotropic (directional) variograms could not be analyzed because of an insufficient number of data for some directions.

Three models of theoretical variograms (gaussian, hemispheric and exponential) and two adjustment methods (OLS and Weighted Least Squares (WLS)) were also assayed. Root mean squared error (RMSE) was used for selection of the best model for the structure of spatial variation, selecting models that produced lowest RMSE in cross validation. Geostatistical analyses were carried out with *gstat* package (Pebesma, 2004).

Model assessment

To assess predictive performance of model we employed a cross validation approach, based on the results of the leave-one-out method, two types of statistics were derived. The leave-one-out method is an iterative process where, for each step an observation is excluded from the data set, the remaining observations being used to fit the model and calculate an estimate value for the excluded datum. This process is repeated for every observation in the data set. The two statistics used for evaluation of predictive capability of models were RMSE and the coefficient of determination (R^2) of predicted vs. observed values. RMSE was calculated as follows:

$$\text{RMSE} = \sqrt{\frac{1}{n} \sum_{i=1}^n (\hat{z}_i - z_i)^2} \quad (3)$$

where \hat{z}_i was the predicted WSC on the i^{th} plot and (z_i) , the observed WSC on the i^{th} plot.

To assess the relative error reduction (RER) of the regression kriging (RMSE_k) estimate in relation to that obtained by linear regression (RMSE_r), the following proportion was calculated (Sales et al., 2007):

$$\text{RER} = (\text{RMSE}_r - \text{RMSE}_k) / \text{RMSE}_r \quad (4)$$

Another statistic used for comparison of the performance of both approaches was the determination coefficient (R^2) calculated by adjusting a simple linear regression model between the observed data and data estimated in the cross-validation. A low RMSE value or a close to one value of R^2 would indicate a better predictive capability of the model.

Estimation of WSC for the Cuitzeo basin

An interpolation was made for estimating the values of woody biomass in the oak forests in the remaining area of the Cuitzeo basin, applying the models showing the best performance i.e. least error and largest predictive capability. The total value of woody biomass in oak forests resulting from the interpolation and calibration of satellite images was compared with values obtained through the traditional method i.e. that obtained from the product of the field values (average woody biomass per area) and the total surface area of forests. The relation between WSC values vs. oak patch sizes and Euclidean distance to roads was calculated so as to explore potential differences in WSC for two variables that are more related to anthropic disturbances than to biophysical parameters.

Results

According to the distribution map shown in Fig. 1, the study area includes 27166 ha of oak forests spread over 912 fragments of varying sizes. Among these fragments, 279 are less than 2 ha (occupying 1.2% of the oak-forest area), 208 are between 2 and 4 ha in size (2.2%), 280 are between 4 and 20 ha (9.3%), and 145 are greater than 20 ha (87.3%).

Table 1 contains the basic statistics of some parameters of the structure of the vegetation recorded in the sampled sites. The low average of basal area allows for inferring a high degree of anthropic intervention, which is further confirmed by the high number of sprouts and stools.

Correlation and regression analyses

The linear correlation analysis (see Table 2) shows nearly all spectral bands are correlated with WSC, the red band being noticeable for its high negative coefficient value. The NIR band is the only one having a positive correlation, but only in the scene from December. The NDVI profits on a basic principle for building vegetation indices: vigorous vegetation absorbs energy in the red portion of the spectrum while reflecting large amounts of IR wavelengths. This means that, in general, NDVI has higher correlation values relative to individual bands. Panchromatic band also showed a strong correlation but less than the red band or NDVI.

Texture values show a moderate positive or negative correlation depending on the spectral region, in the former case indicating that areas with high biomass content also have a higher tonal variability in the NIR, the opposite occurring in panchromatic images.

Regarding topographic variables, only elevation had a positive linear correlation value that was significantly different from zero, slope and solar radiation not showing signs of a linear correlation with the analyzed variables. The sign of the correlation coefficient for

Table 1
Basic descriptive statistics of field variables.

	Mean	Minimum	Maximum	Variance
WSC ($t\ ha^{-1}$)	35.28	0.86	87.71	353.26
Basal area ($m^2\ ha^{-1}$)	12.82	0.58	29.23	36.33
Stools ($n\ ha^{-1}$)	402	50	1390	77,605
Sprouts ($n\ ha^{-1}$)	723	65	2900	264,542

Table 2
Linear correlation coefficients between image variables and WSC.

	Scene: 583/310 and 311 (24 December 2009), $n = 61$	Scene: 584/310 and 311 (2 November 2009), $n = 17$
Green	-0.536	-0.646
Red	-0.615	-0.685
NIR	0.289	-0.376
MIR	-0.501	-0.669
Pan	-0.602	-0.656
NDVI	0.702	0.754
Variance (NIR)	0.411	0.254
Dissimilarity (NIR)	0.546	0.455
Variance (Pan)	-0.415	-0.642
Dissimilarity (Pan)	-0.493	-0.661
Elevation	0.388	
Slope	-0.090	
Solar radiation	0.073	

elevation indicates that forests with higher content of woody biomass tend to occur at higher elevations.

The nearly two-month period between dates of acquisition of images (Nov. 2 and Dec. 24) resulted in strong differences in reflectance patterns of forests, making it difficult to transfer results between them, because of which a regression model was adjusted for each date. Fig. 3 shows that the slope of the NDVI–WSC regression of scenes acquired in December is nearly one half of the same from November.

The outlier analysis showed four plots that had a noticeable effect on the model's adjustment. One of these plots represented the condition of having the least aerial woody biomass ($1.16\ t\ ha^{-1}$) in an area of open scrubland, because of which pixel reflectance values did not correspond only to the woody component. The remaining three plots presented mixed structural forest conditions and therefore a high heterogeneity of pixel values. These four plots were not included in further analyses. Regression models with the original response variable showed heteroscedasticity and lack of normality that were eliminated after a square root transformation of the dependent variable.

Spectral variables explained the largest percentage of variation of the regression model, namely the red and NIR bands together or NDVI alone. Due to its higher explanatory power (higher R^2) NDVI was chosen for the WSC model. Considered separately, textural and topographic variables explained 26 and 18% of the variation, respectively, but when added to NDVI, their standard error increased considerably, their contributions becoming not significant, with the single exception of solar

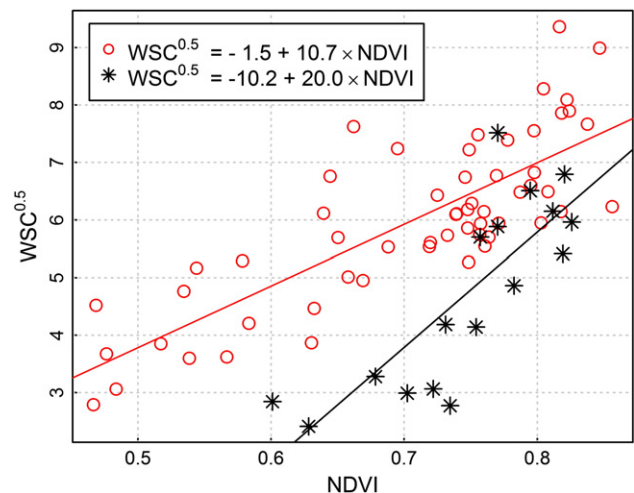


Fig. 3. Observed slope differences between NDVI and WSC due to scene acquisition date. Symbols: (*) = November 2 (scenes 584/310 and 584/311), (°) = December 24 (scenes 583/310 and 583/311).

radiation, which had a null linear correlation with response variables but acted complementarily with NDVI in the regression analysis displaying a diffuse positive relation with WSC. The partial residuals plots shown in Fig. 4 graphically displays the relative contributions of regressors better explaining the variation of the two models; as expected from the correlation analysis, NDVI has a clear and strong positive relation with WSC although the slope values differ between both models. The final linear regression model is presented in Eq. (5). The estimated parameters and their significance tests can be seen in Table 3.

$$(\text{WSC})^{0.5} = \beta_0 + \beta_1 \times \text{NDVI} + \beta_2 \times \text{SR} \quad (5)$$

Geostatistical analysis

The empirical variograms built from the residuals of the regression models clearly show spatial autocorrelation, the variance of residuals increasing with distance between plots reaching an inflection point at approximately 1200 m (see Fig. 5).

The three theoretical models fit the data well, independently of the method employed: OLS or WLS. However, in terms of predictive capability, the best model was obtained by WLS adjustment (option 2 in *gstat*; weight = $N_j/[\gamma(h_j)]^2$), a method having larger range and sill-nugget (see Table 4). The exponential model produced lowest RMSE and was chosen for kriging interpolation (see Fig. 4).

Model evaluation

The results of cross validation for LR and RK are shown in Fig. 6. Incorporation of spatial dependency improves the performance of the model in two ways, decreasing the error and improving predictive capability. Using RK the value of R^2 increased from 0.61 to 0.69. This moderate increment also reduced the error in estimated WSC from 11.01 to 9.77 t ha⁻¹, which represents a RER of 11.3%. In terms of predictive capability, Fig. 6 graphically shows that RK increases the capability for predicting high biomass values. At WSC values close to 80 t ha⁻¹, the value estimated by LR is 60 t ha⁻¹ while RK predicts 74 t ha⁻¹, a figure that is nearer to the observed value.

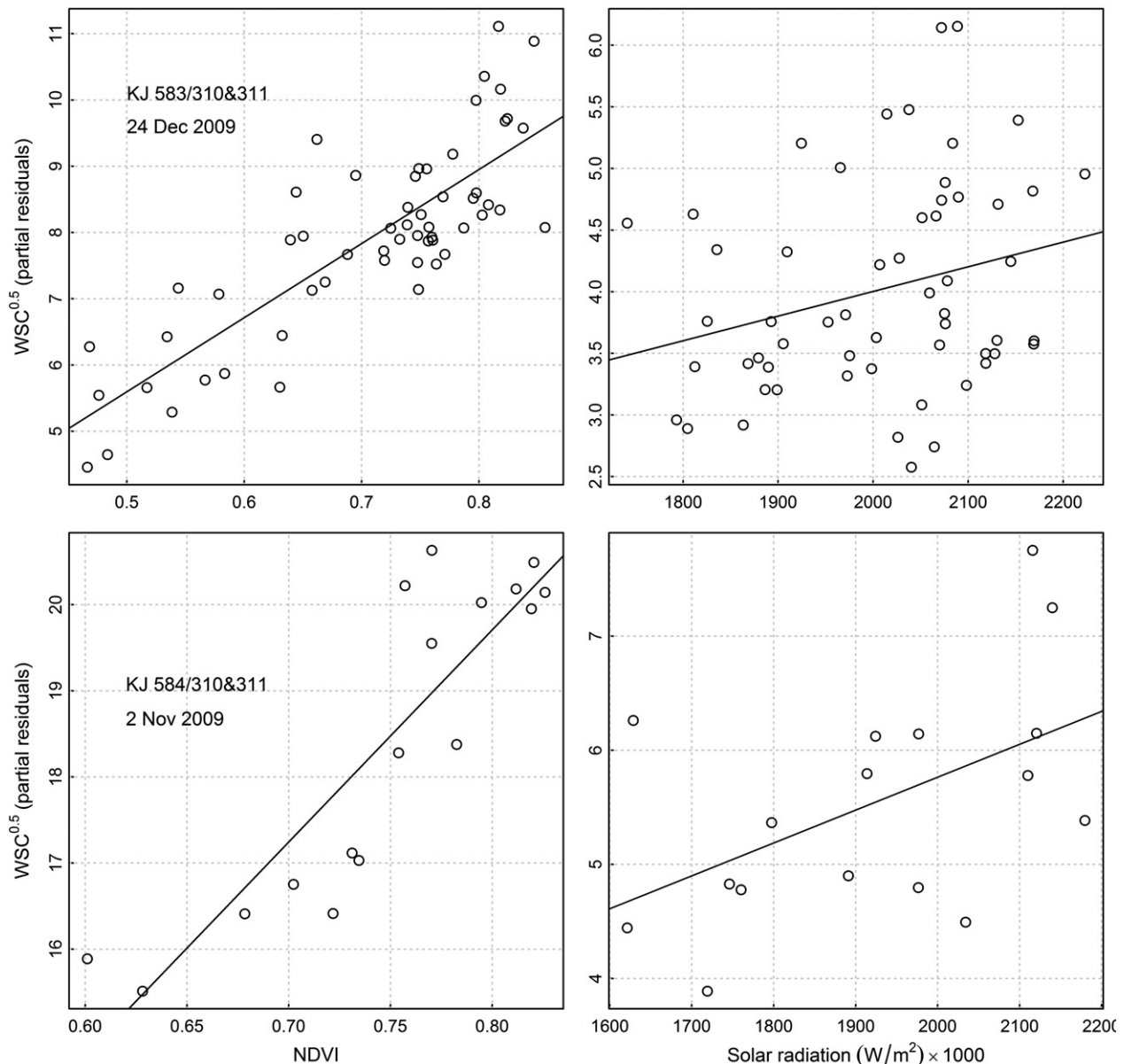


Fig. 4. Partial residuals plots of both images showing contribution of selected variables in regression models.

Table 3
Estimated parameters and significance tests of regression models.

	Scenes: 583/310 and 311 (24 December 2009), n = 57	Scenes: 584/310 and 311 (4 November 2009), n = 17
β_0	-5.926	-19.21
β_1	11.19	24.64
β_2	0.00002001	0.00002882
R^2	0.668	0.715
Probability ($\beta_0 = 0$)	0.0123	0.0038
Probability ($\beta_1 = 0$)	<0.0001	<0.0001
Probability ($\beta_2 = 0$)	0.0490	0.0856
Probability (F-value = 1)	<0.0001	0.0001
Probability (non-normal)*	0.058	0.599
Probability (heteroscedastic)**	0.362	0.856

* Shapiro–Wilk test.
** Breush–Pagan test.

The distribution of estimated woody biomass in the basin and the uncertainty levels of the interpolation is shown in Fig. 7, which highlights that forests with higher woody biomass content are distributed in the mountainous areas in the western portion of the basin, and that the variance of the estimations increases in locations farther away from sampling sites.

The sum of estimated WSC for all pixels in the basin has a value of 704291 ± 39500 t. In comparison, the value estimated by the traditional method (mean of field data multiplied by the area of polygon) is of 958,441 t, which signifies a difference between both estimates of 36.08%. Table 5 shows how WSC average values vary regarding oak patch size and Euclidean distance to roads. As opposite to soil quality, solar radiation or water runoff for example, these two variables are more related to anthropic rather than natural sources of variation in expected values of WSC.

Discussion

Method of interpolation and sources of uncertainty

The precise estimation and distribution of woody biomass content of forests are essential for designing management programs, establishing conservation and/or restoration strategies, and analyzing charcoal supply chains. Until today, despite the ample range of available instruments for forest measurement, and remote sensing data, precise estimation of forest biomass remains an operational challenge

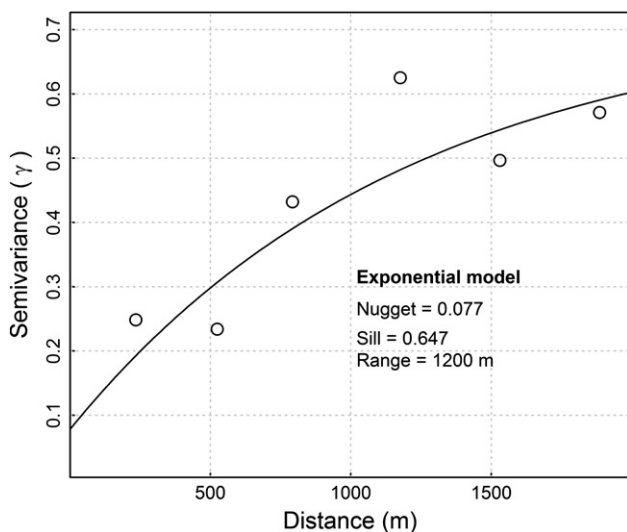


Fig. 5. Plot of experimental and theoretical variograms of residuals.

Table 4
RMSE and parameters of theoretical variograms adjusted according to the ordinary least squared and weighted least squared methods.

Model	Ordinary least squared				Weighted least squared			
	RMSE	Nugget	Sill	Range	RMSE	Nugget	Sill	Range
Gaussian	9.89	0.206	0.376	922.2	9.86	0.191	0.426	1018.5
Spherical	10.0	0.105	0.460	1563.2	9.96	0.099	0.457	1703.6
Exponential	9.84	0.062	0.582	822.5	9.78	0.077	0.647	1201.1

due to the variety of associated sources of error. Chave et al. (2004) group this sources in four types: error due to tree measurement, inadequate size of the study plot, inadequate distribution of sampling sites and the choosing of allometric models. This last type of error will have the largest impact on the uncertainty of the final result of the estimation process. A fifth type of error must be included when spatial distribution is taken into consideration, which is derived from the method chosen for interpolation of field data.

The use of allometric equations using few data or from small trees may involve important sources of error, estimated by Chave et al. (2004) to be in some cases of up to 20%. Another example is that of Cairns et al. (2003), who report biases of up to 31% due to the use of allometric equations not adjusted with local data. These instances are illustrative of the importance of using equations adjusted with enough locally gathered data covering an ample range of tree size classes and to take into account the influence of large trees.

In order to reduce the levels of uncertainty in the present study we used species-specific equations adjusted with local data and the effect of large dimension trees was accounted for. Exponential equations were used that had the best performance for small trees (<31.8 cm dbh) but overestimated the biomass of large trees, for which linear equations were used to avoid such overestimation. Thus, the level of error was sensitively reduced by the combined use of both systems of equations, a strategy deemed as necessary due to the coexistence in managed forests of trees with different architectures.

The difference between the estimation of the total stock of WSC in the Cuitzeo basin by the traditional i.e. based on land cover maps, and the RK methods was of nearly 36%, a figure that illustrates the magnitude of the biased resulting only from choosing the interpolation method. Refinements done to the traditional approach, such as sample stratification and the use of auxiliary information can reduce the differences between estimations derived from both methods; however, RK provides the additional advantage of knowing the variance of the estimation.

Disadvantages of the method applied and independent variables

The use of satellite images is recognized as one of the better alternatives for obtaining confident estimations of forest parameters at the level of landscape, as supported in several studies (e.g. Castillo-Santiago et al., 2010; Lasserre et al., 2011; Lu, 2006). Nevertheless, this approach is not exempt of difficulties one of the most noticeable being to transfer obtained relations between scenes, which in many instances may imply that estimations of forest parameters are only valid for that image for which the model was calibrated, thus limiting the generalization of results to other regions or time periods. Foody et al. (2003) mention some factors limiting this transferability of results including suboptimal conversion of digital levels to reflectance, differences in methods and equations for biomass estimation, differences due to composition and type of vegetation and differences between field data and image acquisition dates.

In our case, despite the fact that all these above-mentioned factors were kept constant we found differences in reflectance patterns of scenes from the two different analyzed tracks, which lead us to assume that such changes were in large part due to phenological changes in oak forests induced by moisture losses. The dry period in

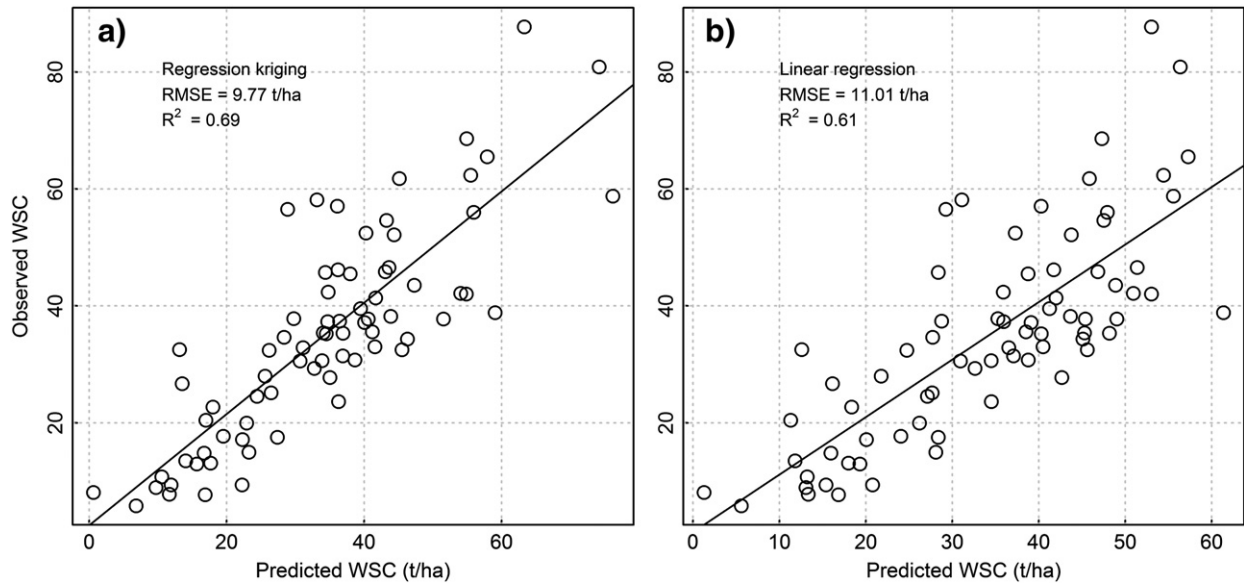


Fig. 6. Cross-validation results of regression kriging (a) and linear regression (b).

the study region usually begins in November and persists until April (García, 2004), because of which the images acquired during November have reflectance values of a forest having a high humidity

content, while December images capture a forests that has experienced moisture loss almost during two months. A follow-up of the reflectance value patterns would be highly useful for arriving to a

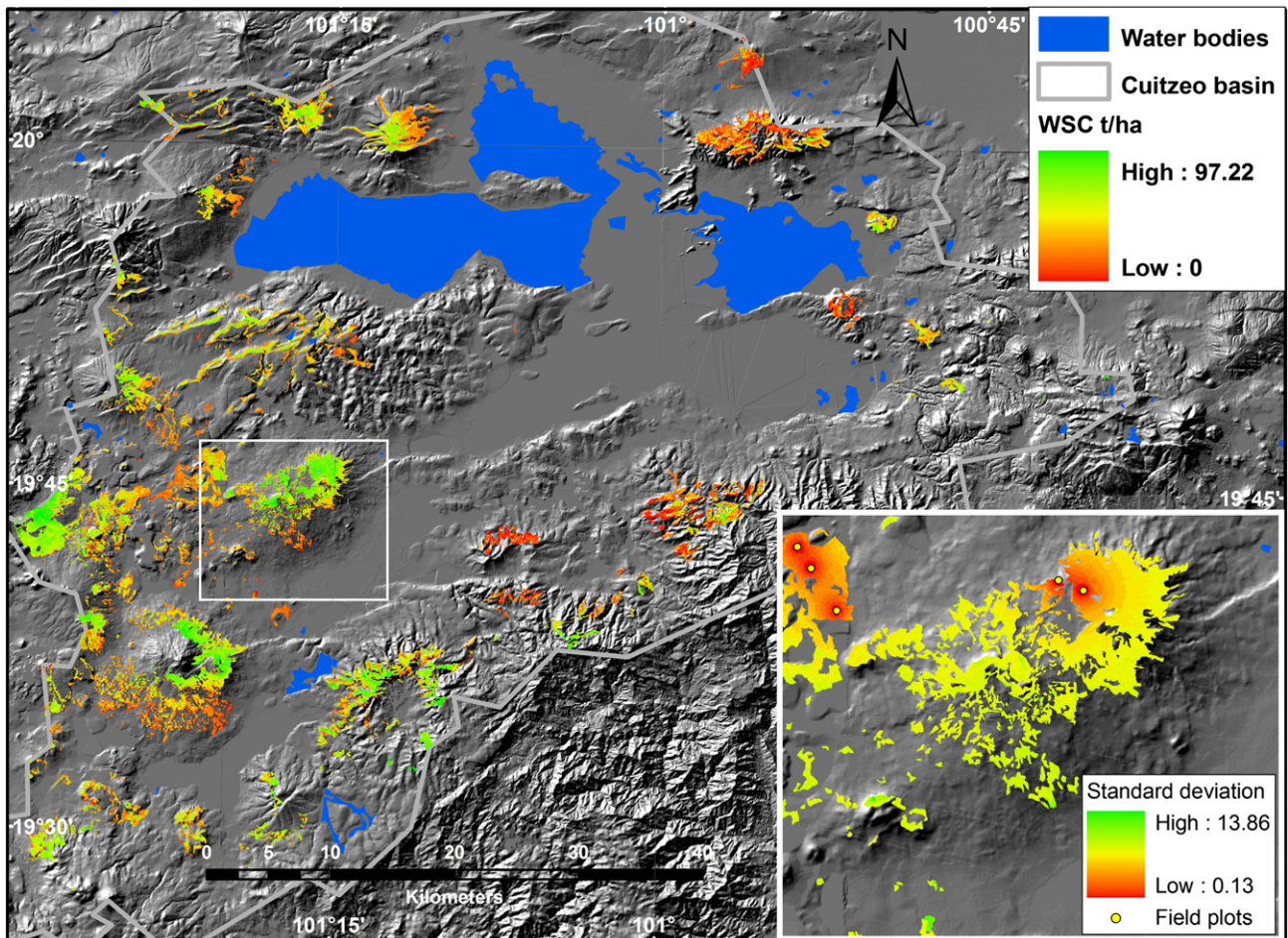


Fig. 7. Spatial distribution WSC in the Cuitzeo basin. An example of the spatial distribution of uncertainty is shown in the bottom right box, the magnified area corresponds to the white rectangle.

Table 5

Mean and total values of WSC regarding the size of oak forest patches and Euclidian distance from roads.

Patch size (ha)	Mean WSC (tDM ha ⁻¹)	Standard deviation	Total WSC per class (tDM)
<20	19.8	14.0	68,178
20–40	20.2	14.4	35,191
40–60	23.2	17.2	22,627
60–80	24.9	14.6	31,498
80–100	26.2	15.0	18,897
> 100	27.7	15.7	527,900
Total			704,291
Distance from roads (m)	Mean WSC (t/ha)	Standard deviation	Total WSC per class (tDM)
<500	23.1	14.3	129,023
500–1000	24.5	14.4	136,281
1000–1500	26.3	15.1	147,188
1500–2000	26.9	16.1	131,087
>2000	29.1	17.7	160,714
Total			705,291

better generalization of the relations obtained in each considered image.

Another highly commented on inconvenience of the use of spectral vegetation indices as biomass predictors is saturation. NDVI frequently shows a linear relation with low biomass levels but after a given biomass threshold value it becomes practically invariable showing an asymptotic behavior. Because of this saturation effect, the use of NDVI is only valid for low biomass content levels at which the biomass–NDVI relation is linear. In the present study, NDVI showed a saturation point around 60 t ha⁻¹ of WSC (see values close to 8 in the y axis of Fig. 3), which limited the predictive capability of the model. Incorporation of other independent variables, above all kriging interpolations, substantially improves the predictive capability. This effect can be easily appreciated in Fig. 6, in which for an observed WSC value of 80 t ha⁻¹, the predicted value using linear regression is of 58 t ha⁻¹ and that using regression kriging is of 74.2 t ha⁻¹. Our results agree with those from other studies demonstrating an improvement in the accuracy of biomass estimates through the use of spatial interpolation methods (Sales et al., 2007).

Recently, the utility for estimating vegetation attributes of spatial information contained in remote perception images (e.g., texture) has been highlighted. Texture is a non-spectral variable with a documented relation to biomass that has been shown to be highly explanatory in different contexts (Castillo-Santiago et al., 2010; Lu, 2006), however, in our case although it was moderately correlated with woody biomass it did not provide significant information to the regression model, mainly because of its collinearity with NDVI. However, it is worthy to comment about the nature of the obtained relations of texture in the correlation analysis. In the NIR band, texture was positively correlated while in the panchromatic band the correlation was negative. This apparent contradictory outcome is due to vegetation reflecting large part of the energy from the NIR electromagnetic region but very little from the visible region, thus in the panchromatic band integrated by visible green and red wavelengths the forests show little tonal variation and hence, low texture values.

About the results

The representation of the spatial distribution of biomass is a tool for visualizing the continual variation of the contents of WSC in space, which widens its application for further analyses as compared to an aggregated value. For example, relations with other biophysical and/or anthropic spatially explicit variables can be evaluated, or the design of sustainable management practices can be coupled with landscape planning tools and spatial dynamic models (Costanza and Voinov, 2004;

Deaton and Winebrake, 2000; Murayama and Thapa, 2011; Paegelow and Camacho-Olmedo, 2008). It can be readily seen from Fig. 7 that low values of WSC are more prone to be distributed over the patchier or fragmented oaklands. This is also shown in Table 5, along with Euclidean distances to roads. In this regard, accessibility to oak patches seems to be correlated with lower-than-expected values of WSC. However, the available information and the results from the present analysis are not enough to prove this spatial pattern, neither the cause for this eventual “man-driven variation”, WSC must vary with biophysical conditions given topography, geomorphology, soil type, solar radiation, among others. A thorough understanding of naturally driven variations in WSC is first needed before moving forward in the search for anthropic-driven variations.

The share of charcoal production in WSC variations eventually driven by human activities is not clear neither given current available data. As mentioned above, oaklands in the study area are mostly used for charcoal production; however, lower values of WSC can be caused indirectly by other human activities such as grazing—and to a lower extent—fuelwood collection for local markets.

Despite these limitations, some insights can be drawn regarding the sustainability of current practices given charcoal demand and wood supply estimates in the study area. When comparing the total estimated WSC in the Cuitzeo basin (704,291 tDM) with the expected annual demand range (11315–23385 t yr⁻¹), and assuming 1) no forest growth (i.e. no coppicing), 2) charcoal as the only use of oak wood, and 3) no other land use land cover change drivers, between 30 and 62 years would be needed for stock depletion. Of course this is an unrealistic scenario as oaks coppice readily, but gives a quantitative idea of an extreme value. Accounting for a ground-based estimation of the annual sustainable production potential of oak wood is not a simple task, and exceeds the objectives of the present study. For example, growth rates from coppicing and seedlings—such as those reported by Aguilar et al. (2012) for the same study area—need to be integrated by GIS analysis and modeling. The carrying capacity of WSC and coppice-shoot density at any location given biophysical constraints needs to be estimated as well. Moreover, growth functions and assumptions in Aguilar et al. (2012) can only be applied to similar biophysical subregions within the Cuitzeo basin, meaning that new chronosequences will be needed if growth estimates are to be assigned to varying locations. However, the spatial distribution of WSC presented in this study is an important starting point towards a spatially-explicit estimation of the annual sustainable production potential of oak wood.

According to Aguilar et al. (2012), between 81% and 89% of the aboveground woody biomass (AGB) of trees is used for charcoal making, so our representation is also indirectly showing the spatial distribution of the AGB, which is a valuable input as regards carbon offset projects under REDD or similar national initiatives.

Conclusions

The approach used here, based on the use of satellite images, digital elevation models and modeling incorporating spatial autocorrelation of field data is shown to be a reliable alternative for estimating the values of woody biomass contents in forests. Modeling of the spatial autocorrelation of field data allowed overcoming a well-known problem of spectral data, saturation of vegetation indices.

Beyond these above-mentioned positive issues of the method applied, a significant percentage of variation unaccounted by the model, still remains, together with difficulties to transfer results between images from different dates of acquisition. Regarding the former complication, other sources of data may contribute to reduce errors in the models, for example, images captured during the dry and the wet seasons and having a higher spectral resolution, such as from Landsat. The use of light detection and ranging (LIDAR) and interferometric radar for estimating the vertical structure of vegetation has also

proved to be of great aid for improving the predictive capability of biomass estimation models, but their high cost unfortunately remains to hamper the frequent use of the techniques. Result transferability between images issues can also represent a serious limitation; however, an adequate distribution of field sampling plots may attenuate many of the encountered problems.

The analysis allowed not only for total accounting of the current stock of available woody biomass suitable for charcoal but more important, its distribution in space. However, to evaluate changes in time, a multi-temporal analysis is needed which poses a methodological challenge as ground data are not available for past years (e.g. Ryan et al., 2012). In any case, future estimations based on new ground data and updated satellite images will allow for an evaluation of temporal trends in WSC. Finally, to determine eventual impacts of charcoal production in the future availability of WSC, more studies are needed that include other uses of oakwood; although charcoal making is the main oakwood product by far. A very promising option is to build *what-if* scenarios using GIS-based modeling techniques that incorporates all the known parameters from the production, transport, selling and end-use (i.e. the charcoal value chain), and account for land use land cover changes due to multiple drivers not necessarily related to wood energy.

Acknowledgments

We thank the Instituto Nacional de Estadística y Geografía (INEGI)—Mexico for their help during the orthorectification of satellite imagery, Hugo Zavala (CIGA-UNAM) for technical assistance and Sergio Zárate for providing language help and writing assistance. A. Fernández received a scholarship from UNAM, Mexico. This research was funded by a research grant managed by K. Oyama: “Conservation status of oak forests in the *Cuitzeo* basin” and a ClimateWorks grant: “Addressing Forest Degradation in Mexico through REDD+”. Role of the funding source: The funding sources (ClimateWorks, UNAM scholarship and K. Oyama’s grant) had no involvement in the study design; in the collection, analysis, and interpretation of data; in the writing of the report; and in the decision to submit the paper for publication.

Appendix A. Supplementary data

Supplementary data to this article can be found online at <http://dx.doi.org/10.1016/j.esd.2012.10.007>.

References

Aguilar R, Ghilardi A, Vega E, Skutsch M, Oyama K. Sprouting productivity and allometric relationships of two oak species managed for traditional charcoal making in central Mexico. *Biomass Bioenergy* 2012;36:192–207.

Ahrends A, Burgess ND, Milledge SAH, Bulling MT, Fisher B, Smart JCR, et al. Predictable waves of sequential forest degradation and biodiversity loss spreading from an African city. *Proc Natl Acad Sci U S A* 2010;107:14556–61.

Arnold M, Köhlin G, Persson R, Shepherd G. Fuelwood revisited: what has changed in the last decade? Center for International Forestry Research (CIFOR). Indonesia: Bogor Barat; 2003.

Arnold JEM, Köhlin G, Persson R. Woodfuels, livelihoods, and policy interventions: changing perspectives. *World Dev* 2006;34:596–611.

Avitabile V, Herold M, Henry M, Schmullius C. Mapping biomass with remote sensing: a comparison of methods for the case study of Uganda. *Carbon Balance Manage* 2011;6:7.

Cairns MA, Olmsted I, Granados J, Argaez J. Composition and aboveground tree biomass of a dry semi-evergreen forest on Mexico’s Yucatan Peninsula. *For Ecol Manage* 2003;186:125–32.

Castillo-Santiago MA, Ricker M, de Jong BHJ. Estimation of tropical forest structure from SPOT-5 satellite images. *Int J Remote Sens* 2010;31:2767–82.

Chave J, Condit R, Aguilar S, Hernandez A, Lao S, Perez R. Error propagation and scaling for tropical forest biomass estimates. *Philos Trans R Soc Lond B Biol Sci* 2004;359:409–20.

Clark DB, Clark DA. Landscape-scale variation in forest structure and biomass in a tropical rain forest. *For Ecol Manage* 2000;137:185–98.

Costanza R, Voinov A. Landscape simulation modeling: a spatially explicit, dynamic approach. New York: Springer; 2004.

Deaton ML, Winebrake JJ. Dynamic modeling of environmental systems. New York: Springer; 2000.

Emrich W. Handbook of charcoal making: the traditional and industrial methods. Dordrecht, The Netherlands: D. Reidel Publishing Company; 1985.

FAOStat. ForestStat—forestry statistics. Rome: FAO; 2010 [<http://faostat.fao.org/>].

Foody GM, Cutler ME, McMorrow J, Pelz D, Tangki H, Boyd DS, et al. Mapping the biomass of Bornean tropical rain forest from remotely sensed data. *Global Ecol Biogeogr* 2001;10:379–87.

Foody GM, Boyd DS, Cutler MEJ. Predictive relations of tropical forest biomass from Landsat TM data and their transferability between regions. *Remote Sens Environ* 2003;85:463–74.

Fox J, Weisberg S. An R companion to applied regression. 2nd edition. Thousand Oaks CA: Sage; 2011.

García E. Modificaciones al sistema de clasificación Climática de Köppen. 5th edition. México DF: UNAM; 2004.

Goetz SJ, Baccini A, Laporte NT, Johns T, Walker W, Kellndorfer J, et al. Mapping and monitoring carbon stocks with satellite observations: a comparison of methods. *Carbon Balance Manage* 2009;4:2.

Hansfort SL, Mertz O. Challenging the woodfuel crisis in West African woodlands. *Hum Ecol* 2011;39:583–95.

Haralick RM, Shanmuga K, Dinstein I. Textural features for image classification. *IEEE Trans Syst Man Cybern* 1973;36:610–21.

Hengl T, Heuvelink GBM, Rossiter DG. About regression-kriging: from equations to case studies. *Comput Geosci* 2007;33:1301–15.

Hernandez-Stefanoni JL, Gallardo-Cruz JA, Meave JA, Dupuy JM. Combining geostatistical models and remotely sensed data to improve tropical tree richness mapping. *Ecol Indic* 2011;11:1046–56.

Hofstad O. Woodland deforestation by charcoal supply to Dar es Salaam. *J Environ Econ Manage* 1997;33:17–32.

IEA. World energy statistics and balances (database). International Energy Agency; 2012. <http://dx.doi.org/10.1787/data-00510-en> [Accessed on 09 October 2012].

IEA. Energy for cooking in developing countries. In: OECD/IEA, editor. *World Energy Outlook 2006*. Paris: International Energy Agency (IEA); 2006. p. 419–45.

Im J, Gleason CJ. A review of remote sensing of forest biomass and biofuel: options for small-area applications. *GISci Remote Sens* 2011;48:141–70.

INEGI. XIII Censo General de Población y Vivienda, 2010. México DF: Instituto Nacional de Estadística, Geografía e Informática (INEGI); 2010.

INEGI. Censo de Población y Vivienda 2010. Principales resultados por localidad (ITER), Michoacán de Ocampo. México DF: Instituto Nacional de Estadística y Geografía (INEGI); 2011.

ITT. FLAASH module user’s guide, ENVI-FLAASH Version 4.3. Boulder, CO, USA: ITT Visual Information Solutions; 2006.

Johnson M, Lam N, Brant S, Gray C, Pennise D. Modeling indoor air pollution from cookstove emissions in developing countries using a Monte Carlo single-box model. *Atmos Environ* 2011;45:3237–43.

Khundi F, Jagger P, Shively G, Sserunkuuma D. Income, poverty and charcoal production in Uganda. *For Policy Econ* 2011;73:199–205.

Larsen WA, McCleary SJ. The use of partial residual plots in regression analysis. *Technometrics* 1972;14:781–90.

Lassere B, Chirici G, Chiavetta U, Garfi V, Tognetti R, Drigo R, et al. Assessment of potential bioenergy from coppice forests through the integration of remote sensing and field surveys. *Biomass Bioenergy* 2011;35:716–24.

Legendre P. Spatial autocorrelation—trouble or new paradigm. *Ecology* 1993;74:1659–73.

Lillesand TM, Kiefer RW. Remote sensing and image interpretation. 3rd edition. New York: John Wiley & Sons; 1994. p. 750.

López E, Bocco G, Mendoza M, Velázquez A, Aguirre JR. Peasant emigration and land-use change at the watershed level: a GIS-based approach in Central Mexico. *Agr Syst* 2006;90:62–78.

Lu DS. The potential and challenge of remote sensing-based biomass estimation. *Int J Remote Sens* 2006;27:1297–328.

Lu D, Batistella M. Exploring TM image texture and its relationships with biomass estimation in Rondônia. *Acta Amazonica* 2005;35:249–57.

Masera O, Arias T, Ghilardi A, Guerrero G, Patiño P. Estudio sobre la evolución nacional del consumo de leña y carbón vegetal en México 1990–2024. México DF: Universidad Nacional Autónoma de México (UNAM); 2010.

Mendoza M, Bocco G, Bravo M, López G. Evaluación de la calidad espacial y temporal de estaciones meteorológicas. El caso de la Cuenca del Lago de Cuitzeo. *Ciencia Nicolaita* 2005;39:79–94.

Mendoza M, Bocco G, Bravo M, López M, Osterkamp W. Predicting water-surface fluctuation of continental lakes. A RS and GIS based approach in Central Mexico. *Water Resour Manage* 2006;20:291–311.

Mendoza ME, Granados EL, Geneletti D, Perez-Salicipup DR, Salinas V. Analysing land cover and land use change processes at watershed level A multitemporal study in the Lake Cuitzeo Watershed, Mexico (1975–2003). *Appl Geogr* 2011;31:237–50.

Murayama Y, Thapa RB. Spatial analysis and modeling in geographical transformation process: GIS-based applications. New York: Springer; 2011.

Mwampamba TH. Has the woodfuel crisis returned? Urban charcoal consumption in Tanzania and its implications to present and future forest availability. *Energy Policy* 2007;35:4221–34.

Naughton-Treves L, Kammen DM, Chapman C. Burning biodiversity: woody biomass use by commercial and subsistence groups in western Uganda’s forests. *Biol Conserv* 2007;134:232–41.

Paegelow M, Camacho-Olmedo MT. Modelling environmental dynamics: advances in geomatic solutions. 1st ed. New York: Springer; 2008.

Paradzay C, Annegam HJ. Estimating potential woody biomass in communal savanna woodlands from synthetic aperture radar (SAR). *Int J Appl Geospat Res* 2012;3:53–62.

Parikka M. Global biomass fuel resources. *Biomass Bioenergy* 2004;27:613–20.

Pebesma EJ. Multivariable geostatistics in S: the gstat package. *Comput Geosci* 2004;30:683–91.

- Pennise DM, Smith KR, Kithinji JP, Rezende ME, Raad TJ, Zhang JF, et al. Emissions of greenhouse gases and other airborne pollutants from charcoal making in Kenya and Brazil. *J Geophys Res Atmos* 2001;106:24143–55.
- R Development Core Team. R: a language and environment for statistical computing. Vienna, Austria: R Foundation for Statistical computing; 2012.
- Ryan CM, Hill T, Woollen E, Ghee C, Mitchard E, Cassells G, et al. Quantifying small-scale deforestation and forest degradation in African woodlands using radar imagery. *Glob Chang Biol* 2012;18:243–57.
- Sales MH, Souza CM, Kyriakidis PC, Roberts DA, Vidal E. Improving spatial distribution estimation of forest biomass with geostatistics: a case study for Rondônia, Brazil. *Ecol Model* 2007;205:221–30.
- Stockholm Environment Institute. Charcoal potential in southern Africa: final main report and country reports. Stockholm, Sweden: Stockholm Environment Institute (SEI); 2002.
- Tucker CJ. Red and photographic infrared linear combinations for monitoring vegetation. *Remote Sens Environ* 1979;8:127–50.
- von-Jonstorff HJ, Nagel O. Heat energy and fuels; pyrometry, combustion, analysis of fuels and manufacture of charcoal, coke and fuel gases (reprint of 1923 edition). Charleston, USA: Nabu Press; 2010. p. 322.
- Zulu LC. The forbidden fuel: charcoal, urban woodfuel demand and supply dynamics, community forest management and woodfuel policy in Malawi. *Energy Policy* 2010;38:3717–30.

Allometric equations for coppice-shoots of *Quercus castanea*, *Q. laeta* and *Q. deserticola*.

Exponential model for large trees $a(x)^b$ dbh < 31.8cm

Biomass component		kg in dry matter			
		a	b	SY•X	pseudo-R ²
<i>Q. castanea</i>	Woody biomass suitable for charcoal making (WSC)	0.0324	2.7425	9.7078	0.97
	Residues (foliage and small branches)	0.0103	2.5551	3.3082	0.89
	Total aboveground biomass (AGB)	0.0416	2.7154	11.6339	0.97
<i>Q. laeta</i>	Woody biomass suitable for charcoal making (WSC)	0.0256	2.7206	11.5328	0.92
	Residues (foliage and small branches)	0.0150	2.1318	1.7418	0.80
	Total aboveground biomass (AGB)	0.0333	2.6648	12.8011	0.92
<i>Q. deserticola</i>	Woody biomass suitable for charcoal making (WSC)	0.0085	3.0667	8.5761	0.87
	Residues (foliage and small branches)	0.0101	2.5868	2.6454	0.85
	Total aboveground biomass (AGB)	0.0156	2.9458	10.7189	0.88
<i>Q. spp.</i>	Woody biomass suitable for charcoal making (WSC)	0.0120	3.0357	13.3636	0.92
	Residues (foliage and small branches)	0.0125	2.4628	4.0826	0.78
	Total aboveground biomass (AGB)	0.0187	2.9451	15.7101	0.92

Lineal model for large trees $(a+bx)$ dbh > 31.8cm

Biomass component		kg in dry matter			
		a	b	SY•X	R ²
<i>Q. castanea</i>	Woody biomass suitable for charcoal making (WSC)	-66.3454	9.2996	19.8611	0.87
	Residues (foliage and small branches)				
	Total aboveground biomass (AGB)	-76.9375	10.9048	23.4035	0.87
<i>Q. laeta</i>	Woody biomass suitable for charcoal making (WSC)	-60.9368	7.3762	17.6499	0.80
	Residues (foliage and small branches)				
	Total aboveground biomass (AGB)	-65.7138	8.0538	19.0418	0.81
<i>Q. deserticola</i>	Woody biomass suitable for charcoal making (WSC)	-37.9128	5.1626	11.4664	0.76
	Residues (foliage and small branches)				
	Total aboveground biomass (AGB)	-47.8853	6.6368	14.2244	0.78

<i>Q. spp.</i>	Woody biomass suitable for charcoal making (WSC)	-59.7793	8.0282	22.4838	0.77
	Residues (foliage and small branches)				
	Total aboveground biomass (AGB)	-69.0071	9.4367	25.8174	0.78
